

Measuring protein concentration with entangled photons

Andrea Crespi, Mirko Lobino, Jonathan C. F. Matthews, Alberto Politi, Chris R. Neal et al.

Citation: *Appl. Phys. Lett.* **100**, 233704 (2012); doi: 10.1063/1.4724105

View online: <http://dx.doi.org/10.1063/1.4724105>

View Table of Contents: <http://apl.aip.org/resource/1/APPLAB/v100/i23>

Published by the [American Institute of Physics](#).

Related Articles

Microfluidic-driven viral infection on cell cultures: Theoretical and experimental study
[Biomechanics](#) **6**, 024127 (2012)

Formation of multilayered biopolymer microcapsules and microparticles in a multiphase microfluidic flow
[Biomechanics](#) **6**, 024125 (2012)

Optimization of an electrokinetic mixer for microfluidic applications
[Biomechanics](#) **6**, 024123 (2012)

Shape controllable microgel particles prepared by microfluidic combining external ionic crosslinking
[Biomechanics](#) **6**, 026502 (2012)

In situ pressure measurement within deformable rectangular polydimethylsiloxane microfluidic devices
[Biomechanics](#) **6**, 026501 (2012)

Additional information on *Appl. Phys. Lett.*

Journal Homepage: <http://apl.aip.org/>

Journal Information: http://apl.aip.org/about/about_the_journal

Top downloads: http://apl.aip.org/features/most_downloaded

Information for Authors: <http://apl.aip.org/authors>

ADVERTISEMENT

The advertisement features a green and white background with a pattern of thin, vertical lines. At the top, the text 'AIP Advances' is written in a green, sans-serif font. To the right of this text is a graphic of several orange circles of varying sizes, arranged in a curved path. Below the main text, the words 'Special Topic Section:' are written in a smaller, white font. Underneath that, the words 'PHYSICS OF CANCER' are written in a large, bold, white font. At the bottom left, the text 'Why cancer? Why physics?' is written in a green font. At the bottom right, there is a blue button with the text 'View Articles Now' in white.

Measuring protein concentration with entangled photons

Andrea Crespi,^{1,2} Mirko Lobino,³ Jonathan C. F. Matthews,³ Alberto Politi,³ Chris R. Neal,⁴ Roberta Ramponi,^{1,2} Roberto Osellame,^{1,2} and Jeremy L. O'Brien^{3,a)}

¹*Istituto di Fotonica e Nanotecnologie, Consiglio Nazionale delle Ricerche, Piazza L. da Vinci, 32, I-20133 Milano, Italy*

²*Dipartimento di Fisica, Politecnico di Milano, Piazza L. da Vinci, 32, I-20133 Milano, Italy*

³*Centre for Quantum Photonics, H. H. Wills Physics Laboratory and Department of Electrical and Electronic Engineering, University of Bristol, Merchant Venturers Building, Woodland Road, Bristol BS8 1UB, United Kingdom*

⁴*Microvascular Research Labs, School of Physiology and Pharmacology, Preclinical Vet Building, University of Bristol, Bristol BS2 8EJ, United Kingdom*

(Received 11 April 2012; accepted 11 May 2012; published online 5 June 2012)

Optical interferometry is amongst the most sensitive techniques for precision measurement. By increasing the light intensity, a more precise measurement can usually be made. However, if the sample is light sensitive entangled states can achieve the same precision with less exposure. This concept has been demonstrated in measurements of known optical components. Here, we use two-photon entangled states to measure the concentration of a blood protein in an aqueous buffer solution. We use an opto-fluidic device that couples a waveguide interferometer with a microfluidic channel. These results point the way to practical applications of quantum metrology to light-sensitive samples. © 2012 American Institute of Physics. [<http://dx.doi.org/10.1063/1.4724105>]

Even the most advanced sensors are bound by a hard limit in precision—the shot noise or standard quantum limit (SQL) that arises from statistical fluctuations. In a conventional optical interferometer, for example, the precision with which an unknown optical phase ϕ can be measured is limited to $\delta\phi = 1/\sqrt{N}$, where N is the (average) number of photons used to probe ϕ .^{1–6} Increasing N is usually possible, by increasing laser power for example. However, in some scenarios, the practical limits of laser power are reached and increasing the integration time will reduce the bandwidth of the measurement below that required—gravity wave interferometers are a key example.⁷ In other scenarios, the sample to be measured may be sensitive to light, such that one would like to minimise the photon flux or total number of photons that the sample is exposed to in order to reach the required precision; put another way, one wishes to gain the maximum information allowable by the laws of physics for a given perturbation of the sample. It is this latter scenario that we are focussed on here. By harnessing quantum superposition and entanglement the SQL can be overcome—quantum metrology enables the more fundamental Heisenberg limit of precision, $\delta\phi = 1/N$, to be reached.¹ However, practical applications of quantum metrology require that samples of interest are integrated with quantum optical circuits.

We use the optofluidic device shown in Fig. 1, consisting of a microfluidic channel that passes through one arm of a Mach-Zehnder interferometer (MZI), fabricated by femtosecond laser micromachining.^{8–10} This device combines the stability of integrated optics for high visibility quantum and classical interference^{11,12} with high precision handling of fluid samples.^{8,13} When a solution is fed into the microfluidic channel, any relative phase shift of light (and thereby concentration-dependent refractive index) in the sensing arm

with respect to that acquired in the reference arm can be estimated from the interference fringes.

The period of the interference fringes and the measurement precision $\delta\phi$ depend on the particular state of light used to probe the sample. For classical states of light $\delta\phi \geq 1/\sqrt{N}$, the SQL. Going beyond this limit requires quantum states of light; the canonical example is the NOON state $(|N0\rangle + |0N\rangle)/\sqrt{2}$, which can achieve super-sensitivity and saturate the Heisenberg limit $\delta\phi = 1/N$. Here, super-resolution results in a fringe periodicity that is $1/N$ times shorter than the one obtained with classical light.¹ The generation and detection of NOON states with large N is an active area of research.^{14–16} We test the operation of our device for the $N=2$ NOON state, which enables super-sensitivity and super-resolution, and can be generated from two single photons input into a beamsplitter.¹⁷ Photon losses in the interferometer reduce the measurement sensitivity, making NOON states non-optimal in general.¹⁸ However, for a two-photon input, the NOON state is optimal, since it corresponds to the two-photon Holland-Burnett state,¹⁹ known to be more resilient to losses.²⁰

The device (Fig. 1) was fabricated by femtosecond laser micromachining in a fused-silica sample to enable the integration of optical waveguides^{9,22} and microfluidic channels^{23,24} in a three-dimensional architecture.¹⁰ Waveguides with slightly elliptical cross section were fabricated by astigmatic shaping of the writing laser beam²⁵ so that a small birefringence is induced to preserve linear polarization; the microchannel was fabricated by irradiating a double pyramidal structure followed by etching in a hydrofluoric acid solution in order to have perfectly vertical walls.^{21,23,24}

Photon pairs at $\lambda = 785$ nm were generated via spontaneous parametric down-conversion (SPDC) in a nonlinear bismuth borate BiB_3O_6 (BiBO) crystal²¹ and collected into polarization maintaining fibres (Fig. 1(a)). The photon pairs were coupled into the MZI via fiber arrays. Hong-Ou-Mandel

^{a)}Electronic mail: Jeremy.O'Brien@bristol.ac.uk.

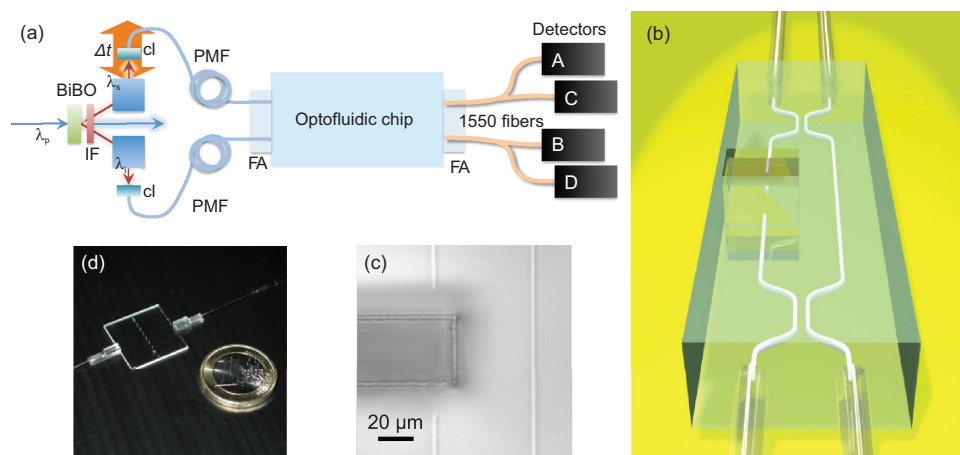


FIG. 1. Quantum metrology in an optofluidic device. (a) Schematic of the experimental setup: A pump laser at $\lambda_p = 392.5$ nm generates pairs of downconverted photons at $\lambda_s = \lambda_t = 785$ nm in a BiBO crystal. IF: interference filter, cl: collection lenses, PMF: polarization maintaining fibers, and FA: fiber array. (b) Schematic of the MZI interfaced to the microchannel. The fluidic channel has rectangular cross-section $500 \mu\text{m} \times 55 \mu\text{m}$ and extends from the top to the bottom surface of the glass substrate (~ 1 mm thickness). The MZI consists of two 50:50 directional couplers and has two arms of equal geometrical length; one waveguide crosses perpendicular to the microchannel, while the other passes externally. (c) Top image of the optical-fluidic interface. (d) Picture of the device with several interferometers and microchannels on chip, together with the fiber arrays for coupling input and output light.

(HOM) interference^{26,27} at the first directional coupler generates a two photon NOON state¹⁷ $(|20\rangle + |02\rangle)/\sqrt{2}$ which is the state we use to probe the sample. Before interfering in the second directional coupler, the sensing mode acquires a relative phase shift in the microchannel that crosses the sensing arm of the MZI.

Output photons are collected by an array of standard telecommunication fibres (monomodal at 1550 nm wavelength, but multimodal at the 785 nm wavelength used), in order to increase collection efficiency, and detected by four single-photon avalanche photodiodes (A, B, C, and D in Fig. 1(a)), after non-deterministic separation at two 50:50 fiber-splitters. With this detection scheme, we are able to monitor the different two photon components of the output state $|11\rangle$, $|20\rangle$ and $|02\rangle$ and renormalize the measured fringes with respect to drifts during the measurement in the coupling between fiber arrays and MZI and source pair production rate.²¹

To establish the quality of quantum interference in our device, we performed a HOM experiment,²⁶ filling the microchannel with distilled water. A lossless MZI composed of two 50:50 couplers, with a relative phase shift ϕ between the two arms, is equivalent to a beamsplitter of reflectivity $\cos^2(\phi/2)$. However, asymmetric losses between the interferometer arms limit the maximum visibility to:

$$V_{HOM} = \frac{4T - (T - 1)^2}{(T + 1)^2}, \quad (1)$$

where T is the transmissivity across the microchannel, equivalent to the ratio of the transmissivity of the two arms and $\phi = \pi/2$.

Figure 2 shows a typical two-photon detection rate across the two output modes as a function of the relative arrival time, controlled with a translation stage (Fig. 1(a)). The visibility $V = 86.7 \pm 1.3\%$ is almost ideal for a ratio of transmissivity $T = 61\%$ since an upper bound of 88% is calculated from Eq. (1). We note that it is merely a coincidence that insertion of distilled water at room temperature in the

channel results in $\phi = \pi/2$ to within the precision of this measurement.

To test the operation of our device with a real sample, we chose bovine serum albumin (BSA) in aqueous buffer solutions as a model fluidic sample that is stable and well-characterized.²⁸ Insertion of the solution in the microchannel was achieved by casting a droplet on the top aperture and exploiting spontaneous filling by capillary action. This geometry is chosen for its simplicity and extension to more sophisticated microfluidic delivery of the solution is straightforward.¹³

We performed sensing measurements using one photon and two photon inputs for 15 different concentrations of BSA ranging from 0% to 7% in 0.5% steps. Cleaning of the microchannel with deionized water and acetone was performed before and after each measurement. The single photon fringe is obtained by coupling only one photon from the SPDC pair into the MZI and counting the number of detections from one output of the MZI. Figure 3(a) shows the single photon count rate normalized with respect to the sum of the singles from the two outputs²¹ together with theoretical fit function $N_{|10\rangle} = (1 + V_{1ph} \cos(\phi + \phi_0))/2$, where V_{1ph} is the fringe visibility, $\phi = \alpha C$ (with C concentration of BSA and α constant), and ϕ_0 is a constant phase offset term.

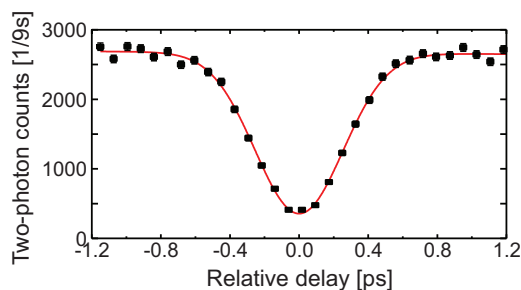


FIG. 2. Quantum interference in the Mach-Zehnder interferometer when the microfluidic channel is filled with distilled water. The coincidences at the detectors A and B are plotted as a function of the relative delay between the two photons.

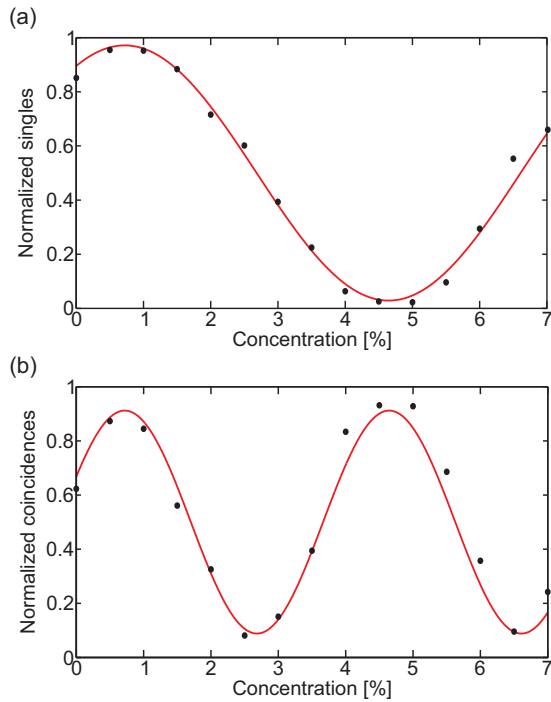


FIG. 3. Quantum interference fringes. Normalized single photon counts (a) and two photon coincidences (b) for different concentrations of bovine serum albumin in a buffer solution (full circles). The solid line represents a fitting of the experimental points with a sinusoidal curve. Error bars on data points are the same size of the dots and computed assuming Poissonian statistics of the detection events; other errors, arising for example from evaporation, are not taken into account. A slight disagreement of the experimental points with the fitting function is attributed to thermal fluctuation and solvent evaporation during the measurement.

A visibility $V_{1ph} = 94 \pm 2.2\%$ is estimated from the fit, compared to a theoretical prediction $V_{theory,1ph} = 97\%$, calculated taking into account the device losses.

Two photon fringes were measured by coupling photon pairs into the two input waveguides of the MZI and detecting coincidences from the two separate output channels. Coincidence events $C_{|11\rangle}$ are normalized with respect to the sum of all the possible two photon outputs²¹ $C_{|11\rangle} + C_{|20\rangle} + C_{|02\rangle}$ and shown in Fig. 3(b) together with the theoretical fit function

$$N_{|11\rangle} = \frac{(1 + V_{2ph} \cos(2\phi + \tilde{\phi}_0))}{2}, \quad (2)$$

where the period is half that of the single photon fringe due to super-resolution. The visibility of the fit is $V_{2ph} = 82 \pm 4.8\%$, in agreement with the theoretical prediction for the interferometer including losses $V_{theory,2ph} = 88\%$. This value exceeds the threshold for supersensitivity:^{29,30} $V_{2ph}^{SQL} = 70.7\%$. Nevertheless, this value does not include source and detector efficiencies which prevent current experiments to beat the standard quantum limit.³¹ In addition to the 2.1 dB ($T = 61\%$) loss across the microfluidic channel, we estimate 0.5 dB propagation losses and 0.5 dB bending losses, which further increase the visibility threshold.

The refractive index change Δn_s of the BSA solution can be related to the phase shift ϕ , acquired by light during propagation in the sample, according to:

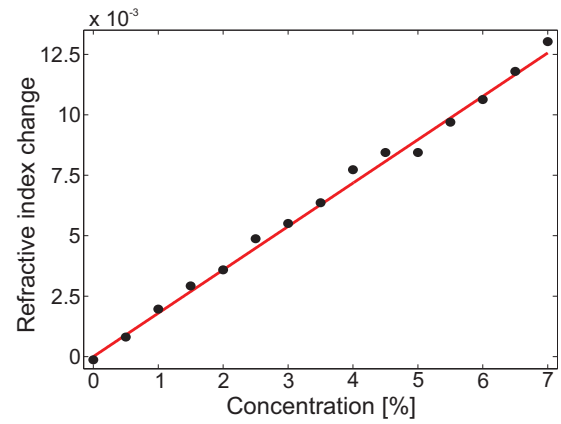


FIG. 4. Refractive index change in the buffer solution as a function of BSA concentration. Experimental data (dots) are shown together with a linear fitting (solid curve).

$$\Delta n_s = \frac{\lambda}{2\pi L} \phi, \quad (3)$$

where $L = 55 \mu\text{m}$ is the microchannel length and $\lambda = 0.785 \mu\text{m}$ is the wavelength. The dependence of Δn_s on the BSA concentration C (Fig. 4) can thus be inferred from the two-photon coincidences reported in Fig. 3. The experimental points are well fitted by a linear function, whose slope $dn_s/dC = 1.79 \pm 0.04 \times 10^{-3}$ is in very good agreement with the value of 1.82×10^{-3} , previously reported³² at $\lambda = 0.578 \mu\text{m}$.

Measurement of the concentration of a protein in solution with entangled states in an integrated quantum photonics device shows the potential for quantum interferometric measurement of light sensitive samples. Heralded or deterministic generation of larger entangled states will enable greater sensitivity,¹⁶ when combined with high efficiency photon sources and detectors. Quantum optical circuits that herald the generation of up to four photon entangled states for quantum metrology have been demonstrated with lithographic waveguides.¹⁵ Multipass schemes⁵ would be compatible with the optofluidic architecture demonstrated here, provided low loss switches can be integrated. More sophisticated microfluidic delivery systems could be integrated for particular applications.^{8,13} Adding more waveguide capabilities, for example, polarization-based quantum measurements,^{3,33} would enable measurement of samples that induce a concentration dependent rotation of the probing light polarization.

This work was supported by the Italian Grant PRIN 2009, EPSRC, ERC, QUANTIP, PHORBITECH, Nokia, and NSQI. M.L. acknowledges a Marie Curie IIF. J.L.OB. acknowledges a Royal Society Wolfson Merit Award.

¹V. Giovannetti, S. Lloyd, and L. Maccone, *Science* **306**, 1330 (2004).

²P. Walther, J. W. Pan, M. Aspelmeyer, R. Ursin, S. Gasparoni, and A. Zeilinger, *Nature (London)* **429**, 158 (2004).

³M. W. Mitchell, J. S. Lundeen, and A. M. Steinberg, *Nature (London)* **429**, 161 (2004).

⁴T. Nagata, R. Okamoto, J. L. O'Brien, K. Sasaki, and S. Takeuchi, *Science* **316**, 726 (2007).

⁵B. L. Higgins, D. W. Berry, S. D. Bartlett, H. M. Wiseman, and G. J. Pryde, *Nature (London)* **450**, 393 (2007).

⁶J. F. C. Matthews, A. Politi, A. Stefanov, and J. L. O'Brien, *Nat. Photonics* **3**, 346 (2009).

- ⁷K. Goda, O. Miyakawa, E. E. Mikhailov, S. Saraf, R. Adhikari, K. McKenzie, R. Ward, S. Vass, A. J. Weinstein, and N. Mavalvala, *Nat. Phys.* **4**, 472 (2008).
- ⁸C. Monat, P. Domachuk, and B. J. Eggleton, *Nat. Photonics* **1**, 106 (2007).
- ⁹R. R. Gattass and E. Mazur, *Nat. Photonics* **2**, 219 (2008).
- ¹⁰R. Osellame, V. Maselli, R. M. Vazquez, R. Ramponi, and G. Cerullo, *Appl. Phys. Lett.* **90**, 231118 (2009).
- ¹¹A. Politi, M. J. Cryan, J. G. Rarity, S. Yu, and J. L. O'Brien, *Science* **320**, 646 (2008).
- ¹²A. Laing, A. Peruzzo, A. Politi, M. R. Verde, M. Halder, T. C. Ralph, M. G. Thompson, and J. L. O'Brien, *Appl. Phys. Lett.* **97**, 211109 (2010).
- ¹³G. M. Whitesides, *Nature (London)* **442**, 368 (2006).
- ¹⁴I. Afek, O. Ambar, and Y. Silberberg, *Science* **328**, 879 (2010).
- ¹⁵J. F. C. Matthews, A. Politi, D. Bonneau, and J. L. O'Brien, *Phys. Rev. Lett.* **107**, 163602 (2011).
- ¹⁶H. Cable and J. P. Dowling, *Phys Rev Lett* **99**, 163604 (2007).
- ¹⁷J. G. Rarity, P. R. Tapster, E. Jakeman, T. Larchuk, R. A. Campos, M. C. Teich, and B. E. A. Saleh, *Phys. Rev. Lett.* **65**, 1348 (1990).
- ¹⁸M. A. Rubin and S. Kaushik, *Phys. Rev. A* **75**, 053805 (2007).
- ¹⁹M. J. Holland and K. Burnett, *Phys. Rev. Lett.* **71**, 1355 (2003).
- ²⁰U. Dorner, R. Demkowicz-Dobrzanski, B. J. Smith, J. S. Lundeen, W. Wasilewski, K. Banaszek, and I. A. Walmsley, *Phys. Rev. Lett.* **102**, 040403 (2009).
- ²¹See supplementary material at <http://dx.doi.org/10.1063/1.4724105> for details on the device fabrication, single photon source, normalization procedure and optimal MZI configuration.
- ²²G. Della Valle, R. Osellame, and P. Laporta, *J. Opt. A, Pure Appl. Opt.* **11**, 013001 (2009).
- ²³A. Marcinkevičius, S. Juodkazis, M. Watanabe, M. Miwa, S. Matsuo, H. Misawa, and J. Nishii, *Opt. Lett.* **26**, 277 (2001).
- ²⁴K. C. Vishnubhatla, N. Bellini, R. Ramponi, G. Cerullo, and R. Osellame, *Opt. Express* **17**, 8685 (2009).
- ²⁵R. Osellame, S. Taccheo, M. Marangoni, R. Ramponi, P. Laporta, D. Polli, S. De Silvestri, and G. Cerullo, *J. Opt. Soc. Am. B* **20**, 1559 (2003).
- ²⁶C. K. Hong, Z. Y. Ou, and L. Mandel, *Phys. Rev. Lett.* **59**, 2044 (1987).
- ²⁷G. D. Marshall, A. Politi, J. C. F. Matthews, P. Dekker, M. Ams, M. J. Withford, and J. L. O'Brien, *Opt. Express* **17**, 12546 (2009).
- ²⁸T. Peters, *The Plasma Proteins* (Academic, 1975).
- ²⁹K. J. Resch, K. L. Pregnell, R. Prevedel, A. Gilchrist, G. J. Pryde, J. L. O'Brien, and A. G. White, *Phys. Rev. Lett.* **98**, 223601 (2007).
- ³⁰R. Okamoto, H. F. Hofmann, T. Nagata, J. L. O'Brien, K. Sasaki, and S. Takeuchi, *New. J. Phys.* **10**, 073033 (2008).
- ³¹A. Datta, L. Zhang, N. Thomas-Peter, U. Dorner, B. J. Smith, and I. A. Walmsley, *Phys. Rev. A* **83**, 063836 (2011).
- ³²R. Barer and S. Tkaczyk, *Nature (London)* **173**, 821 (1954).
- ³³L. Sansoni, F. Sciarrino, G. Vallone, P. Mataloni, A. Crespi, R. Ramponi, and R. Osellame, *Phys. Rev. Lett.* **105**, 200503 (2010).